Energy Engineering

Tech Science Press

https://doi.org/10.32604/ee.2026.087667

ARTICLE

Development of a Bidirectional DC-to-DC Converter with Adaptive Reconfiguration and Battery Heating Capability

Indira Damarla[1], Subhojit Dawn[1,*], Ramudu Ganji[2], Venmathi Mahendran[3] and Taha Selim Ustun[4,*]

[1]Electrical and Electronics Engineering, Siddhartha Academy of Higher Education Deemed to be University, Vijayawada, Andhra Pradesh, India
[2]Electrical and Electronics Engineering, Aditya University, Surampalem, India
[3]Electrical and Electronics Engineering, St. Joseph's College of Engineering, OMR, Chennai, India
[4]Fukushima Renewable Energy Institute, Koriyama, Japan

*Corresponding Authors: Subhojit Dawn. Email: subhojitdawn@vrsiddhartha.ac.in;
Taha Selim Ustun. Email: tahaselim@yahoo.com

Received: 21 June 2026; Accepted: 14 September 2026; Published: 12 November 2026

ABSTRACT: The performance of an electric vehicle (EV) is significantly influenced by environmental conditions, particularly temperature variations. However, this problem has already been addressed, and currently, there are various topologies for heating the battery. These topologies have their own problems, such as high complexity in controlling the system, problems associated with circulating currents, complexity in terms of hardware, and low efficiency. Furthermore, under extremely low-temperature conditions, conventional battery heating systems may experience reduced heating effectiveness because of the temperature-dependent characteristics of batteries and power electronic components. This paper is about an advanced design of a reconfigurable bidirectional DC-to-DC converter that can be used for heating the battery efficiently and resolving problems such as switching stress, complexity in controlling the system, gain, and efficiency using advanced technology. By optimizing transformer and resonant settings, the system achieves a compact structure that is perfect for on board EV integration. By facilitating a faster and more reliable temperature rise, the heating system guarantees dependable operation even in severely cold regions. The recommended converter also features a wider input voltage range, smooth startup, and integrated overcurrent protection. Results obtained from the MATLAB Simulink simulation show that there is improved voltage regulation, increased efficiency, and better usability at low temperatures than in traditional systems, thereby increasing the practicality and reliability of the system.

KEYWORDS: Electric vehicle; bidirectional DC–DC converter; resonant converter; battery heating; soft switching; frequency modulation

1 Introduction

The rapid shift towards the adoption of sustainable modes of transportation in the world has led to an increase in interest in electric automobiles as a green and energy-efficient alternative to conventional internal combustion engine-powered automobiles. Some of the benefits of electric automobiles include reduced greenhouse gases, quiet operation, and high efficiency. The rise in environmental concerns and pollution regulations is driving the electric vehicle segment in both passenger and freight applications in the automobile industry. Power electronics have a significant role to play in enabling electric vehicles and electric modes of transportation [1].

Copyright © 2027 The Authors. Published by Tech Science Press. This work is licensed under a Creative Commons Attribution 4.0 International License, which permits unrestricted use, distribution, and reproduction in any medium, provided the original work is properly cited.

The different battery topologies used for EVs are discussed in detail. The most general battery topology used for EVs is the lithium-ion battery [2]. These batteries retain their efficiency and compactness but also provide the requisite capacity for energy storage in modern EVs. It is observed that the performance characteristics of Li-ion batteries are significantly affected by how they operate and the environment they operate in, mostly temperature, even with all their strengths. The electrochemical reactions in Li ion batteries are found to be significantly reduced at low temperatures, especially below 0°C. This is primarily attributed to the increase in internal resistance and the reduction in available capacity and power capability of the battery at low temperatures [3]. The limits in driving range and acceleration capabilities directly affect the performance of EVs due to the decreased battery capacity. Low-temperature charging of Li-ion batteries may lead to the development of lithium plates on the anode surface, a hazardous process that may destroy the battery [4]. Furthermore, the temperature requirements of the battery must be adhered to so that efficient and safe functioning of the EV is facilitated. Battery thermal management systems have been developed to efficiently control the temperature of the battery during operation [5].

Various battery heating technologies have been proposed to solve the problems the battery is exposed to in low-temperature conditions. Battery heating technologies can be classified into the following types: internal battery heating and external battery heating. Heating pads, plates, or jackets are generally used in external heating techniques for the improvement of the temperature of the battery module [6]. Since it is necessary for the generated heat to pass through the casing of the battery before it reaches the layers of the electrochemical cell, it has often been observed that even though it is simple to apply this technique, it suffers from low heating rates as well as non-uniformity in temperature distribution. The internal heating techniques make use of electric current for generating heat within the cells of the batteries by making use of the internal resistance of the batteries [7]. This technique is able to provide fast rates of heating as well as uniformity in temperature distribution. Alternating-current (AC) heating systems have drawn a lot of interest among internal heating approaches because they minimize electrochemical side reactions while producing efficient heating. AC excitation improves long-term dependability and safety by lowering the risk of lithium plating and excessive battery aging as compared to direct-current (DC) heating techniques [8].

To improve heating efficiency while preserving safe operating conditions, a number of AC-based battery self-heating circuits and resonant heating techniques have been developed [9]. Effective power conversion is a crucial component of EV powertrain systems, along with battery heat management. In order to control power flow between the high-voltage traction battery, auxiliary loads, and charging infrastructure, DC–DC converters are frequently utilized [10]. Because they permit energy to flow in both directions, bidirectional DC–DC converters are especially crucial for features like battery charging, regenerative braking, and vehicle-to-grid (V2G) energy transfer [11]. However, battery heating circuits and power conversion circuits are often built independently in typical EV architectures, increasing the number of components, the size of the system, and the total cost of the system [12]. Resonant DC-DC converters have attracted significant interest in power electronic devices of EVs due to their ability to achieve high efficiencies along with soft-switching capabilities at higher frequency rates. The Inductor–Inductor–Capacitor (LLC) resonant DC–DC converter has been widely used in onboard charger applications due to its soft-switching operation, which helps reduce switching losses and electromagnetic interference (EMI), while various converter topologies have been developed to meet different application requirements [13].

Efficient topologies of the LLC converter have been introduced for its improved performance in terms of efficiency and voltage range [14]. However, it is important to note that the LLC converters have a limited voltage gain capacity. This is attributed to changes in their state of charge as well as dynamic operating conditions. This limitation becomes significant in EV battery applications, where the battery voltage varies over a wide range with the state of charge and dynamic operating conditions, requiring the converter to

provide a wide voltage gain range [15]. There are various techniques used to avoid this hindrance. Some of the converter configurations include capacitor-inductor-capacitor-inductor (CLCL), capacitor-inductor-inductor-capacitor-inductor (CLLCL), and various hybrid resonant converters [16]. These converters have improved the gain capacity of the circuit architecture by increasing the number of resonant circuit components [17]. Although the converters have improved the gain capacity of the converter, they require several passive components as well as a complex control system [18]. The complexity of the converter circuit architecture has also led to a complex design process, a number of passive components in the circuit, as well as a less compact system [19].

Converter topologies with the ability to sustain a wide voltage gain capacity, thus minimizing hardware complexity and enhancing flexibility, continue to be more and more needed [20]. Recently, reconfigurable resonant converter topologies have been the focus of research as a solution to these problems [21]. Through the use of switching, reconfigurable converters have the ability to adjust the resonant network, thus allowing the converter to adjust the operating parameters in accordance with the operating conditions [22]. This enables the converter to achieve a wide voltage-gain range without requiring additional switch components or complex control strategies [23]. The battery heating capabilities can also be incorporated into the power conversion stage of the converter using reconfigurable resonant converters [24]. This is done using the same resonant converter, thus generating controlled alternating currents for battery heating and not requiring additional hardware [25].

Although several AC battery-heating methods and resonant bidirectional DC–DC converters have been reported, most require separate converters or additional heating circuits, increasing hardware complexity, cost, and system size. Moreover, conventional LLC and resonant converter topologies have limited voltage-gain capability under wide battery voltage variations, making them less suitable for EV applications operating over a broad state-of-charge and temperature range.

These challenges motivate the implementation of the reconfigurable bidirectional resonant DC-to-DC converter incorporating an AC battery-heating function in this paper. By incorporating bidirectional power conversion and battery heating into a single converter design, this converter does not require an additional circuit for heating purposes. Moreover, the converter retains its soft-switching behavior with a wide range of input voltages and achieves higher efficiency of converter integration and lower hardware requirements. The key contributions of the research include:

- Demonstration of the reconfigurable bidirectional resonant converter featuring battery-heating ability.
- Exclusion of additional battery heating hardware and thereby decreasing the complexity of the converter.
- A frequency-based control strategy for smooth transition between power-transfer and heating modes.
- Validation through MATLAB/Simulink simulations and hardware prototype results demonstrating stable operation and soft switching.

2 Proposed Bidirectional Converter Topology

The proposed topology, shown in Fig. 1, is designed for efficient bidirectional power conversion as well as battery heating using a single compact converter. Instead of using separate converters for different functions, the proposed topology utilizes a single power converter for both energy transfer and battery heating, thereby achieving a compact and multifunctional converter. The main component of the proposed topology is an isolated resonant DC–DC converter. The proposed converter enables efficient bidirectional power transfer between the battery and the high-voltage DC bus. The isolated resonant DC–DC converter provides high efficiency and a wide operating range with reduced power losses by utilizing a resonant circuit.

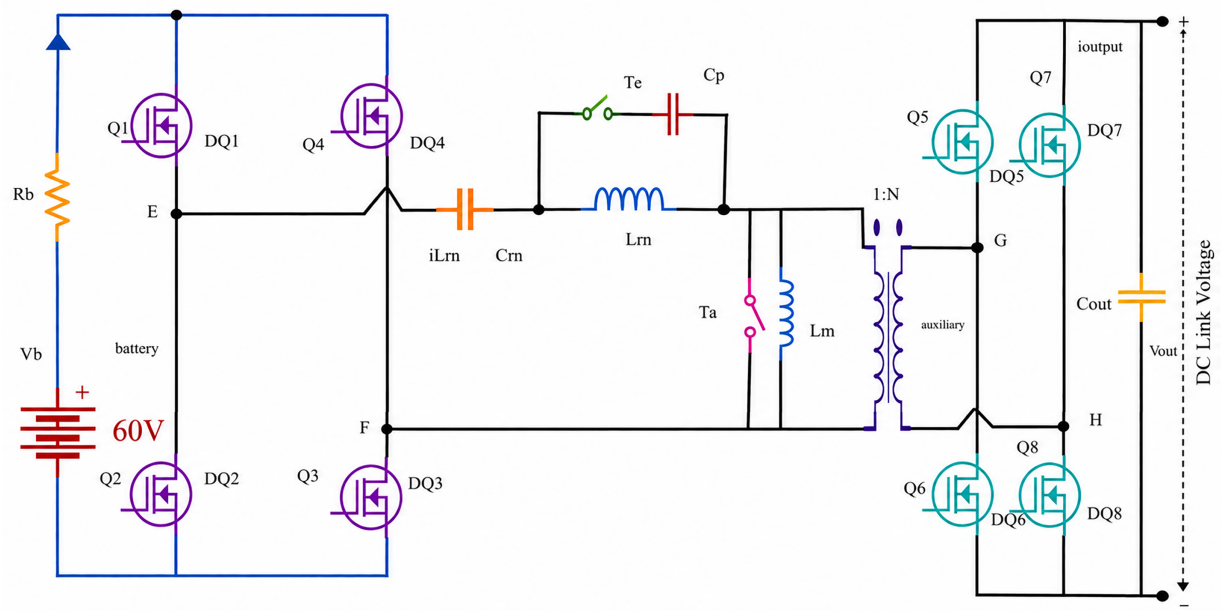


Figure 1: Proposed programmable bidirectional DC-DC converter with battery heating.

The proposed converter integrates bidirectional power transfer and battery heating within a single isolated resonant converter, eliminating the need for a dedicated battery-heating circuit, as shown in Fig. 1. By reconfiguring the switching sequence, the converter operates either in power transfer mode or battery heating mode while utilizing the same resonant tank. This integrated approach reduces hardware complexity, improves power density, and improves the efficiency of the EV power conversion system.

The combination of the resonant inductance, resonant capacitance, and transformer magnetizing inductance determines the operating characteristics of the resonant converter, including its effective resonant frequency and voltage gain profile. Depending on the direction of power flow and the operating 1point relative to the resonant frequency, the converter can achieve soft-switching conditions, such as zero-voltage switching (ZVS) and zero-current switching (ZCS), thereby reducing switching losses. The galvanic isolation provided by the transformer enhances system safety and facilitates compliance with applicable EV safety requirements. Furthermore, the proposed topology can be configured in a modular structure to accommodate different battery voltage levels and power requirements. Therefore, the proposed converter provides a versatile and efficient solution for bidirectional power conversion and battery heating in next-generation electric vehicles.

2.1 Modes of Operation

The proposed reconfigurable bidirectional DC–DC converter operates in two distinct modes: battery heating mode and power transfer mode. The selection of the operating mode is determined by the operating condition of the electric vehicle and the battery temperature. In battery heating mode, the converter is controlled to generate the required alternating current through the battery to facilitate internal resistive heating, whereas in power transfer mode, it enables bidirectional power transfer between the battery and the DC bus.

2.1.1 Power Transfer Mode

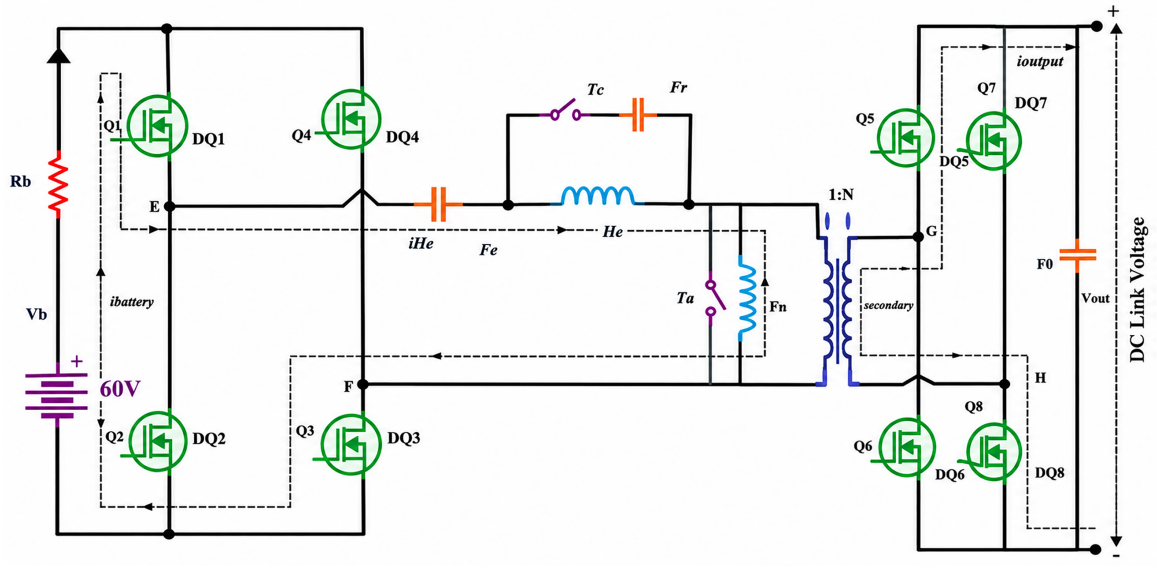
The suggested converter allows the high-voltage DC bus and the battery pack to exchange energy in both directions when in power transfer mode. Regenerative braking situations, regular vehicle propulsion, and grid-connected recharge circumstances all activate this operating mode. The resonant tank is essential to the effective passage of energy between the two ports during this procedure. The converter attains ideal switching conditions that lower switching losses and raise total energy conversion efficiency by operating at the resonant frequency.

The system's battery charging or draining state is determined by the direction of power flow. Fig. 2 shows how the converter operates in power transfer mode. By using this technique, the converter can adapt to the significant variations in battery voltage that often arise from variations in temperature and charge level. During battery draining, electrical energy is transferred to the DC link to power traction motors and other on-board electrical demands shown in Fig. 2a. This maintains effective functioning while reducing conduction losses in the power devices and passive components. The power is moved from the DC link to the battery during the vehicle charging process, reversing the direction of energy flow shown in Fig. 2b. Certain charging patterns must be followed in order to protect battery health and ensure safe functioning. Another advantage of operating near resonance is the reduction of reactive power circulation inside the resonant network. This function improves the converter's energy efficiency and lessens unnecessary current stresses in the components.

During power transfer mode, the converter transfers energy between the high-voltage DC bus and the battery based on the operating mode. This decreases losses during switching, increases the efficiency of the converters, and prevents electromagnetic interference. Since the battery is directly connected to the primary-side full-bridge converter, the instantaneous bridge voltage v_{AB} applied to the resonant tank is equal to $+V_{bat}$ or $-V_{bat}$, depending on the switching state. Thus, the magnitude of the primary-side bridge voltage is given by

$$|v_{AB}| = V_{bat} \tag{1}$$

$$v_{AB} = L_{rn}\frac{d_{irn}}{dt} + V_{cp} + V_L \tag{2}$$



(**a**)

Figure 2: (Continued)

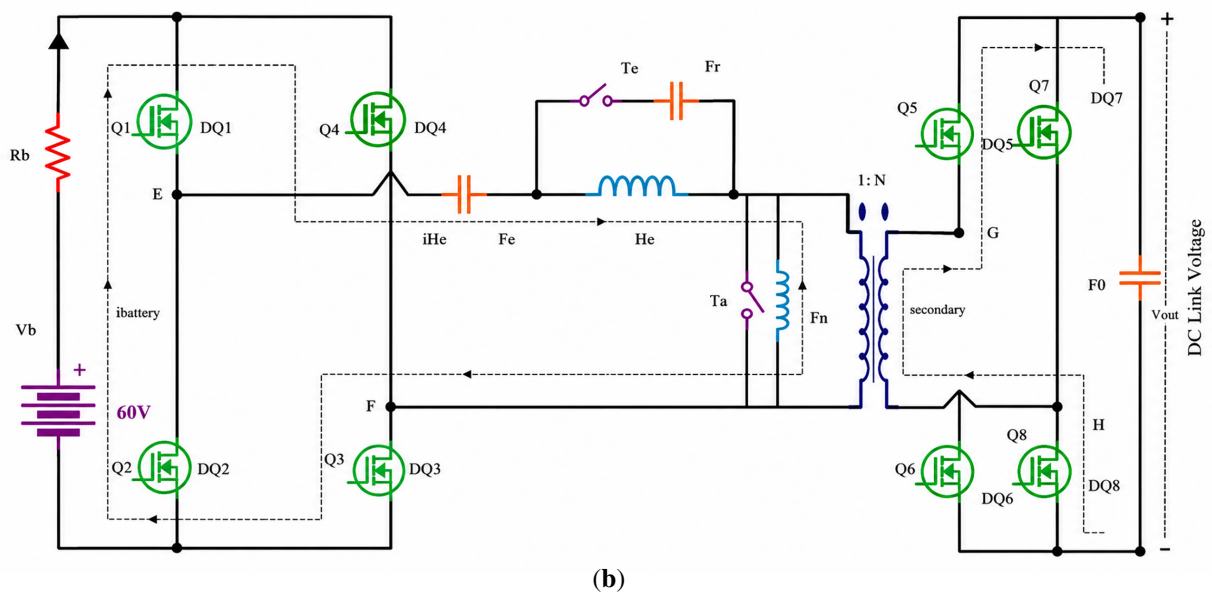


Figure 2: (**a**) Power transfer mode operation: battery to DC-link. (**b**) Power transfer mode operation: DC-link to battery.

2.1.2 Battery Heating Mode

In the case where the battery temperature falls below the predetermined value below which the battery can operate safely, the converter automatically enters the battery heater mode to improve the effectiveness of the battery at low-temperature operation before the commencement of normal charging or traction. Lithium-ion batteries do not perform well at low temperatures because of their slow electrochemical reaction rate and high internal resistance, which causes reduced capacity, output power, and susceptibility to lithium plating during charging.

The present invention utilizes an inherent AC heater built into the converter to increase the temperature of the battery by pumping alternating current into the battery terminals. Under this mode, there is no energy transfer from the converter to any external load or DC bus. Rather, the converter creates resonant current in both the battery and resonant tank to create heat within the battery using its internal resistance. As illustrated in Fig. 3a, switches Q_1 and Q_3 are activated to establish the positive resonant current path, producing a positive heating current through the battery and resonant inductor. During the subsequent half-cycle shown in Fig. 3b, switches Q_2 and Q_4 conduct, reversing the current direction and generating a negative resonant current. Consequently, an alternating current circulates through the battery while maintaining approximately zero average DC current over a switching cycle.

The heat produced in the battery due to its internal resistance is

$$P_{heat} = I_r^2 R_b \tag{3}$$

where I_r = rms value of the injected current and R_b = battery internal resistance.

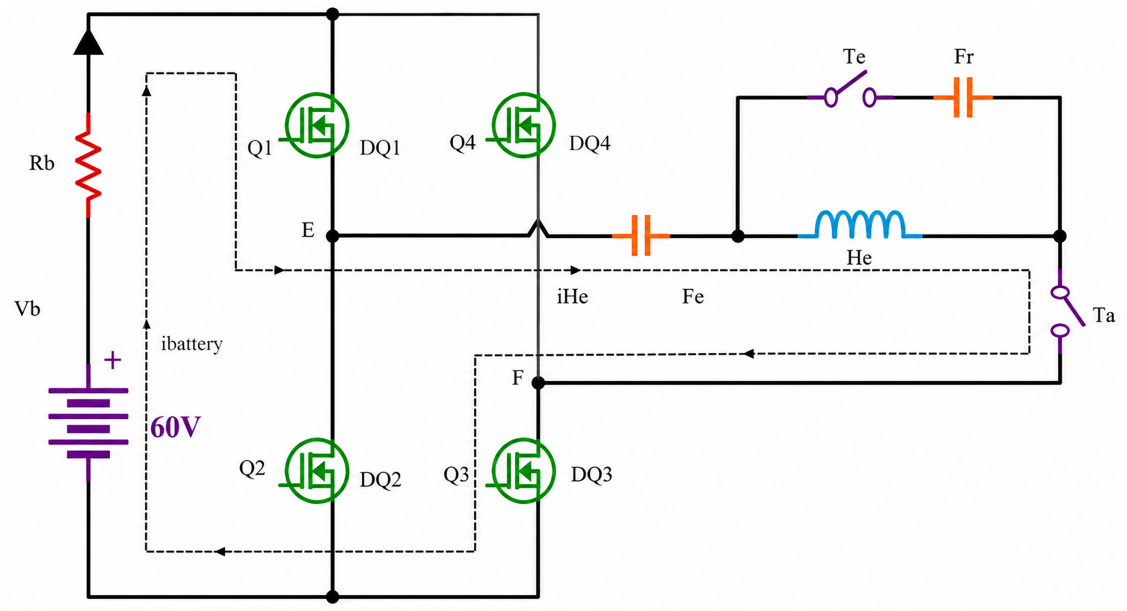
The corresponding battery temperature rise can be estimated using

$$\frac{dT}{dt} = \frac{P_{heat} - Q_l}{mC_p} \tag{4}$$

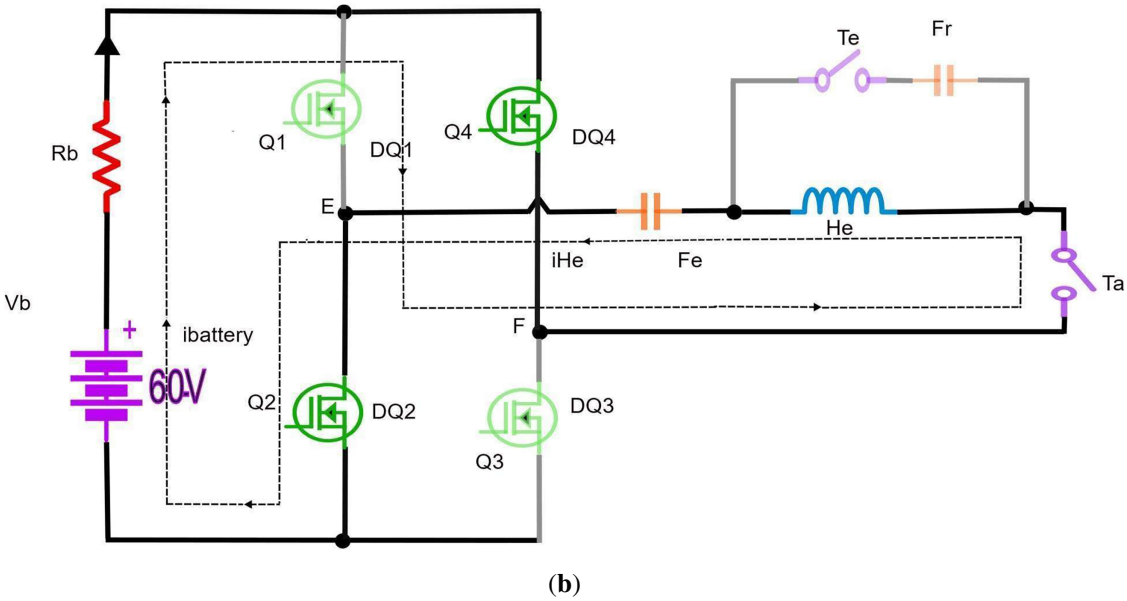
where m is the battery mass, C_p is the effective specific heat capacity of the battery, and Q_l represents the heat dissipated to the surrounding environment.

$$V_{bat} = V_{Cr} + R_{eq} i_{Lr} + L_r \frac{d_{ilr}}{dt} \tag{5}$$

$$V_{bat} = -V_{Cr} - R_{eq} i_{Lr} - L_r \frac{d_{ilr}}{dt} \tag{6}$$



(**a**)



(**b**)

Figure 3: (**a**) Battery heating mode operation: positive resonant current cycle. (**b**) Battery heating mode operation: negative resonant current cycle.

The resonant current

$$I_{Lr}(t) = Ae^{-t}\sin(wt) \tag{7}$$

The heating current

$$I_{RMS} = \sqrt{\frac{1}{T_s}\int_0^{Ts} {i_{Lr}}^2(t)dt} \tag{8}$$

Battery thermal dynamics

$$mc\frac{dT}{dt} + hS\left(T_b - T_o\right) = I_{RMS}^2 R_{\text{int}} + f_r Q_{heat} \tag{9}$$

The heating current magnitude is regulated by varying the converter frequency near to the heating circuit resonance frequency. Working near resonance enhances the amount of heating current and the rate at which the temperature is increased, while working away from the point of resonance decreases the intensity of heating. Although the injected battery current alternates symmetrically around zero within each switching period, resulting in approximately zero average current and negligible net charge transfer, the bidirectional current produces positive power dissipation through the battery's internal resistance. Consequently, the injected AC generates heat inside the battery without causing a significant reduction in state of charge.

The results shown in Fig. 4 show that the proposed heating scheme has been successful in raising the battery temperature ranges −20°C–10°C within 10 min, meaning an approximate rate of 3°C/min. Internal heating makes the battery operate better because of improved electrochemical performance, reduction of internal resistance, and thus enhancing the working of the battery at the low conditions. Hence, the proposed converter facilitates reliable cold start-ups.

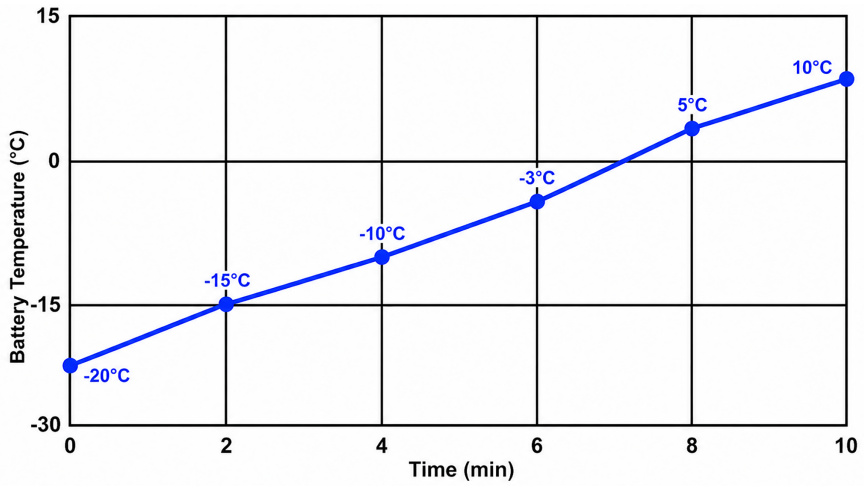


Figure 4: Battery temperature ranges −20°C–10°C within 10 min during battery heating mode.

The performance of the proposed converter was evaluated during the battery preheating stage. The resonant AC current generates heat within the battery, thereby increasing its temperature without causing localized overheating. The proposed heating strategy promotes a uniform temperature distribution throughout the battery pack, which helps reduce thermal stress and preserve the electrochemical performance of the

battery during subsequent charging and discharging operations. The simulation results demonstrate a steady increase in battery temperature without thermal runaway, indicating the suitability of the proposed topology for low-temperature EV applications. The initial and final battery operating temperatures are assumed to be −10°C and 25°C, respectively.

3 Control Strategy of the Proposed Topology

The proposed topology employs the frequency modulation (FM) control strategy to regulate bidirectional power flow and battery heating using a single resonant converter shown in Fig. 5. The operating mode is selected according to the battery temperature and power demand. When the temperature rises above the predefined value, the converter operates in power transfer mode. Otherwise, it switches to battery heating mode to improve battery performance under low-temperature conditions. During mode transition, the switching sequence is gradually modified to avoid voltage and current transients. Appropriate dead time is maintained between complementary switches to prevent shoot-through and ensure reliable converter operation. The battery heating current is controlled by adjusting the switching frequency based on the battery temperature. The resonant current is produced at a higher level at low temperatures for quick heating inside the battery, and the controller decreases the heating current automatically when the battery comes approaches its target operating temperature. The use of this closed-loop control system makes the battery heating process safer and more efficient.

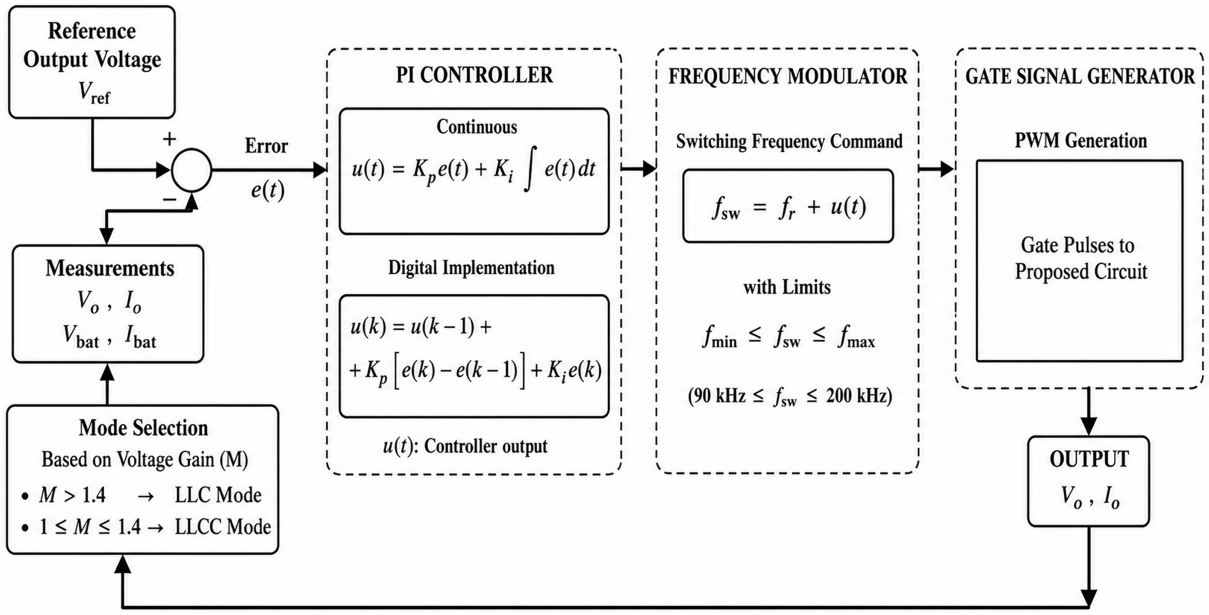


Figure 5: Closed loop control system of the proposed topology.

The switching frequency is determined as

$$f_s = f_r + \Delta f \tag{10}$$

where:

f_r = resonant frequency & Δf = frequency deviation.

The general expression for voltage gain can be evaluated as

$$M(fn) = \left| \frac{V_o}{nV_{in}} \right| \tag{11}$$

The proposed LLC converter gain equation as follows

$$M = \frac{1}{\sqrt{\left[1 + \frac{1}{k}\left(1 - \frac{1}{F_n^2}\right)\right] + Q^2\left(F_n - \frac{1}{F_n}\right)^2}} \tag{12}$$

where:

$$F_n = \frac{f_s}{f_r} \tag{13}$$

for LLC:

$$Z_{io}(jw_{sw}) = \frac{1}{jw_{sw}C_r} + jw_{sw}L_r \tag{14}$$

for LLCC:

$$Z_{io}(jw_{sw}) = \frac{1}{jw_{sw}C_r} + \frac{\frac{1}{jwswC_p}(jw_{sw}L_r)}{\frac{1}{jwswC_p} + jw_{sw}Lr} \tag{15}$$

Fig. 6 illustrates the overall control algorithm adopted for the proposed converter. Frequency modulation is employed to regulate the resonant current while preserving ZVS and ZCS conditions during both power transfer and battery heating operations.

This AC-based heating method gets around the bad electrochemical effects of DC heating and lets the temperature rise quickly and steadily. The switch between heating and power transfer modes is controlled by supervisory control logic. As it can be seen from the above discussion, the flow chart drawn above is a systematic and uniform method for designing an integrated resonant bidirectional converter. This ensures that the designed converter is highly efficient and reliable.

4 Simulation Results and Discussion

To prove the efficiency of the suggested converter design, MATLAB/Simulink simulations and a laboratory model were constructed. The converter was tested in power transfer and battery heating modes to test the validity of the operating principle, resonant characteristics, and soft switching nature. Parameters for simulation of the converter are provided in Table 1 below, whereas the experimental results provide proof of the feasibility of the suggested topology. The experimental model was constructed based on the proposed converter characteristics and worked under the same conditions as the simulation model. The obtained switching waveforms prove the validity of operation of the converter and match the simulated model. The adaptive controller adjusts the switching frequency based on the operating mode and battery voltage. The controller automatically switches to LLC or LLCC mode when required, helping to keep efficiency high over an extended voltage range and operate with zero-voltage switching. The controller is operated with a duty ratio of 0.5, a dead time of 250 ns, and a current limit of 25 A. The converter transitions from LLC to LLCC mode when the voltage increases from 40 to 46 V, while the transition from LLCC to LLC mode occurs when the voltage increases from 46 to 54 V.

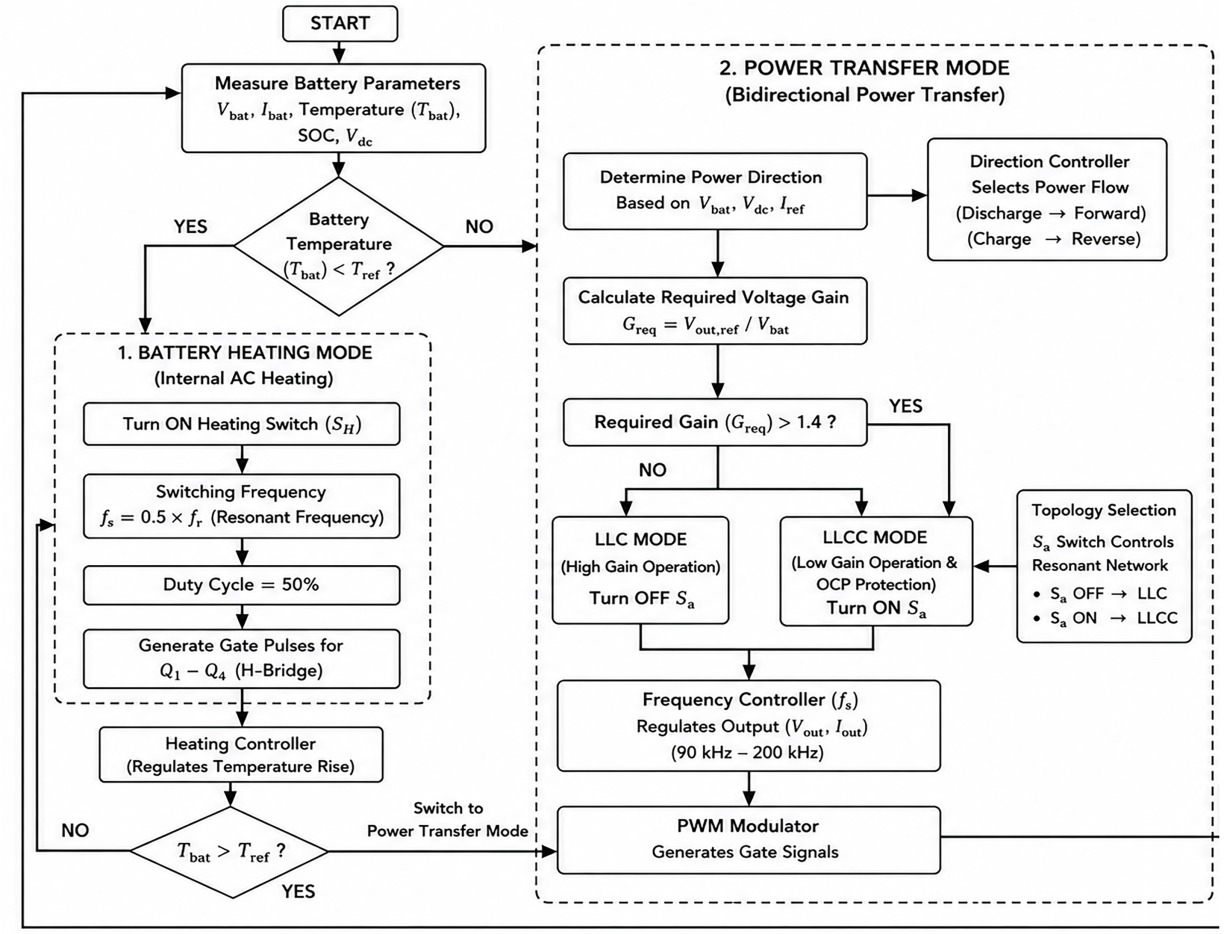


Figure 6: Design and optimization flowchart for the proposed converter. Abbreviations: SOC—state of charge; LLC—Inductor–Inductor–Capacitor; V_{bat}—battery voltage; i_{bat}—battery current; t_{bat}—battery temperature, t_{ref}—reference temperature, i_{ref}—reference current, i_{out}—output current, v_{dc}—DC link voltage, v_{out}—output voltage, LLCC—Inductor–Inductor–Capacitor–Capacitor.

Table 1: Design specifications and parameters.

Parameter	Value
DC Bus Voltage (V_0)	400 V
Battery Side Voltage (V_{in})	160–400 V
Rated Power Output (P)	1 kW
Resonant Frequency (f_{rs})	100 kHz
Magnetizing Inductor	136 μH
Resonant Inductor	33 μH
Resonant Capacitor	90 nF
Parallel Capacitor	20 nF

4.1 Power Transfer Mode

The gate pulses of switch Q_1 and its complementary switch Q_2 are shown in Figs. 7 and 8, ensuring proper half bridge operation. To prevent shot through, an appropriate dead time is kept between the switching transitions. Soft commutation is made possible by this synchronized switching technique, which also lowers switching losses. Complementary operation with switch Q_1 is ensured by the pulse's precise timing and fixed duty cycle. This regulated gating process keeps the power flowing in the right direction and keeps the converter from experiencing shoot-through situations.

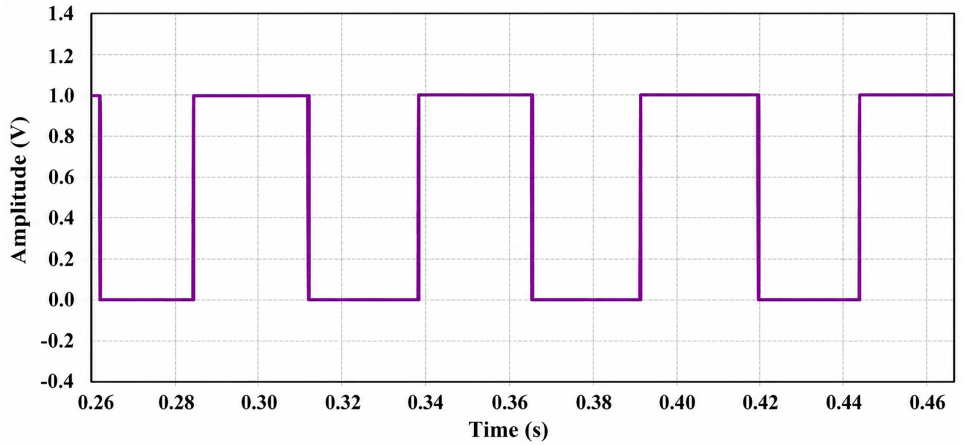


Figure 7: Gate pulse waveform of switch Q_1 during power transfer mode.

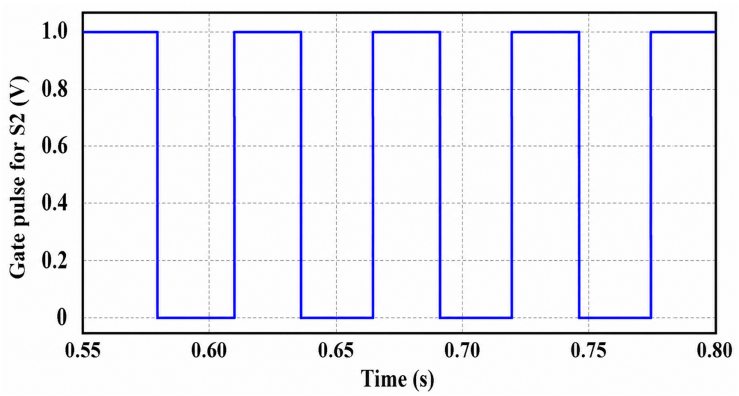


Figure 8: Gate pulse waveform of switch Q_2 during power transfer mode.

The voltage across the switch Q_1 in power transfer mode is shown in Fig. 9. Before the switch is turned on, it is evident that the voltage across Q_1 drops to almost zero. Zero-voltage switching (ZVS) at turn-on is confirmed by this behavior, which greatly lowers switching losses and boosts converter efficiency. The magnetizing inductor current (i_{Lm}) is shown in Fig. 10. In order to prevent core saturation and indicate stable transformer excitation, the waveform keeps its symmetrical triangle shape. This attests to the transformer's appropriate high-frequency functioning design.

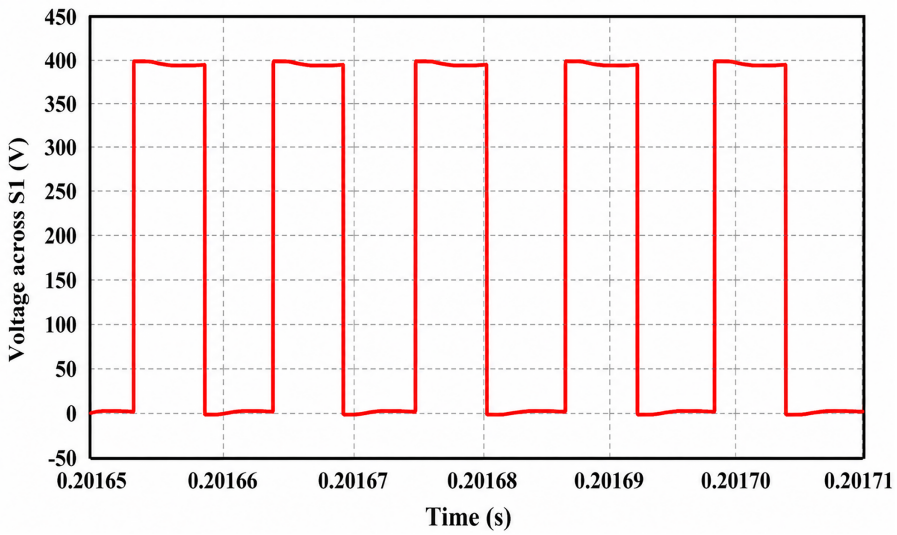


Figure 9: ZVS behavior in voltage waveform across primary-side switch Q_1.

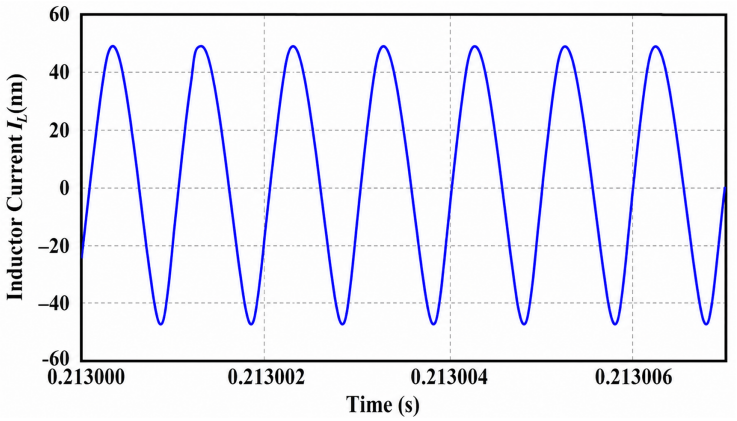


Figure 10: Magnetizing inductor current i_{Lm} during power transfer operation.

4.2 Heating Mode

During the heating mode, the gate signals were applied to switches Q_1–Q_4 and are shown in Figs. 11–14. The resonant tank is excited in both directions by the alternating driving of switch pairs (Q_1, Q_3) and (Q_2, Q_4). For consistent internal heating and lithium plating mitigation, this switching pattern generates a symmetrical alternating current through the battery.

During the heating mode, the proposed converter operates in a reconfigured manner to circulate the current through battery in order to produce internal heat. A resonant tank formed by L_r and C_r ensures controlled AC current injection with reduced switching stress. The resonant inductor current (i_{Lr}) is displayed in Fig. 15.

The near-sinusoidal waveform of the current indicates that the resonant inductor and capacitor are in proper resonance. The resonant tank's efficient operation is confirmed by the smooth current profile, which shows decreased harmonic distortion. Fig. 16 shows the diode current waveform discontinuous conduction with zero current turn-off. The ZCS behavior and lower reverse recovery losses at the transformer secondary side are confirmed when the current generally drops to zero before the diode blocks voltage.

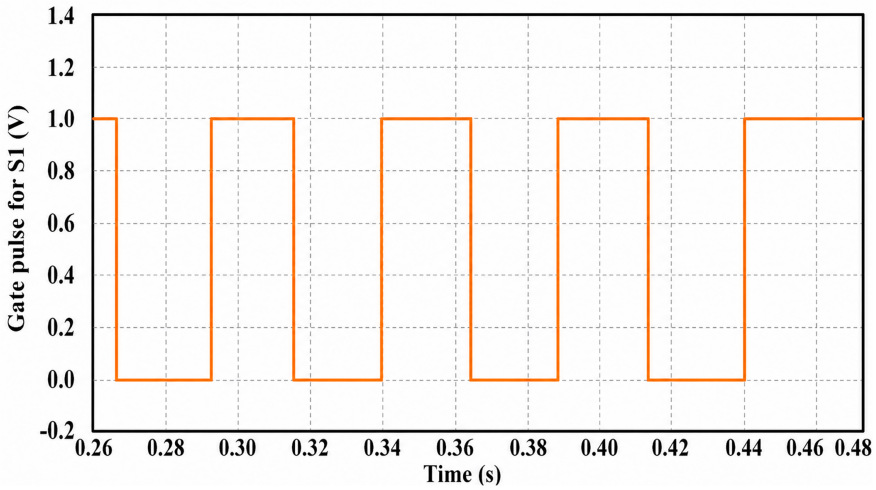


Figure 11: Pulse of switch Q_1 during heating mode.

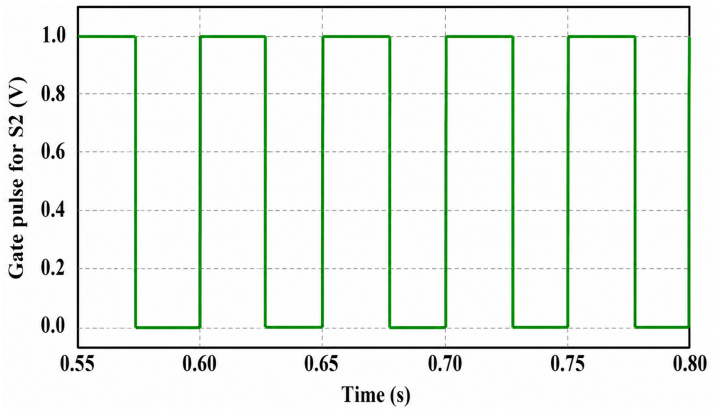


Figure 12: Pulse of switch Q_2 during heating mode.

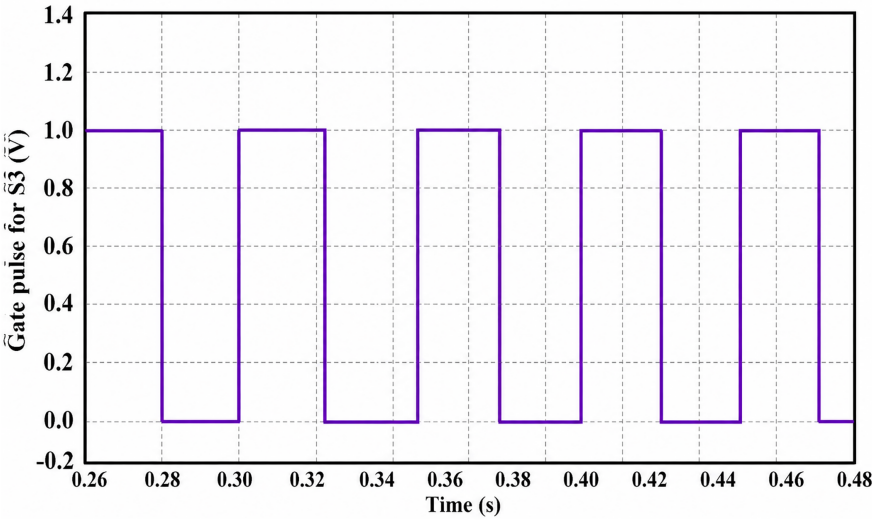


Figure 13: Pulse of switch Q_3 during heating mode.

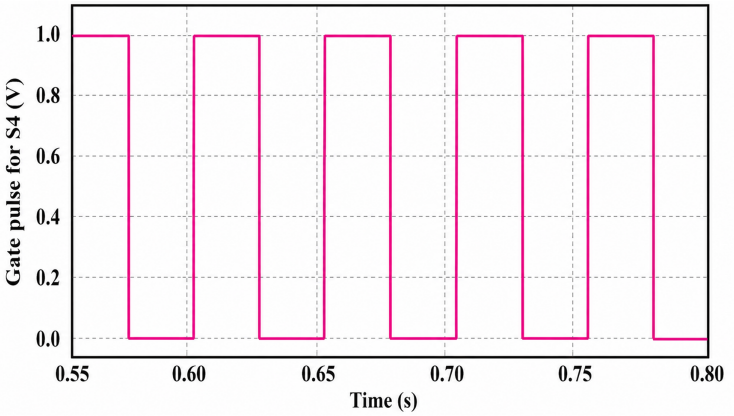


Figure 14: Gate pulse of switch Q_4 during heating mode.

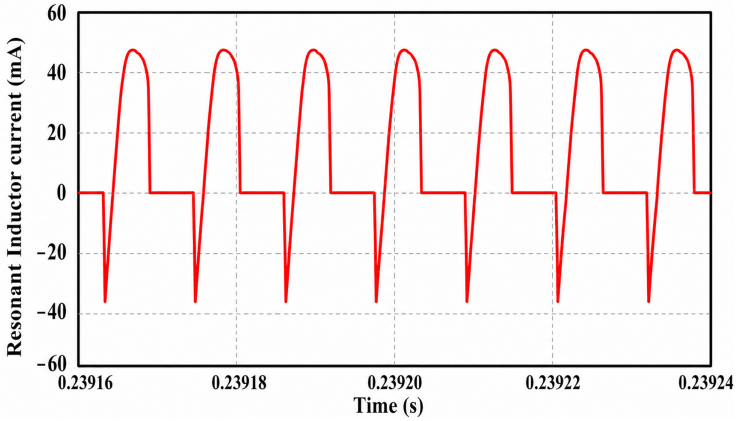


Figure 15: Sinusoidal resonance in resonant inductor current (i_{Lr}).

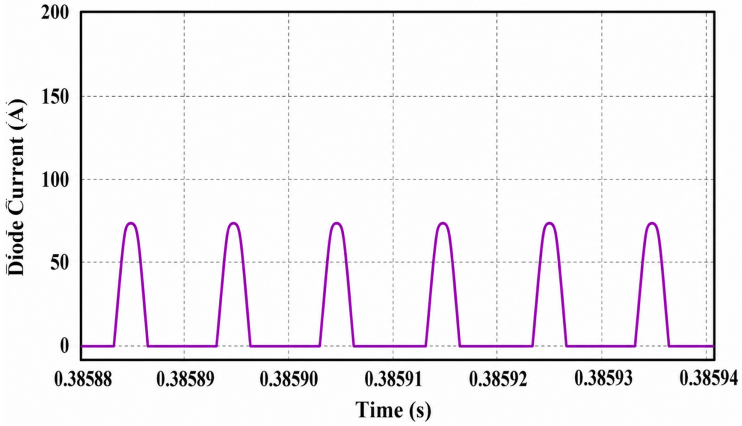


Figure 16: ZCS behavior in the secondary-side diode current.

The switches Q_1 and Q_3 current while the heating process is shown in Figs. 17 and 18. Because of the LC network's resonant tendency, the current has a quasi-sinusoidal character. The seamless current transition

demonstrates reduced switching losses and confirms soft-switching functioning. Safe battery heating is made possible by switching frequency variation, which regulates the current magnitude.

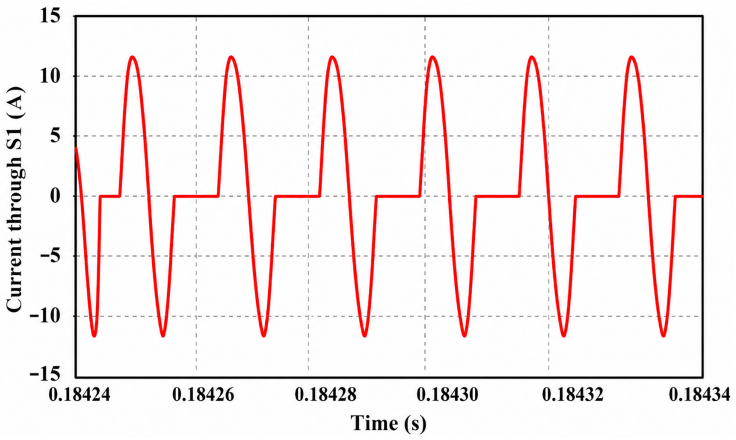


Figure 17: Current through switch Q_1.

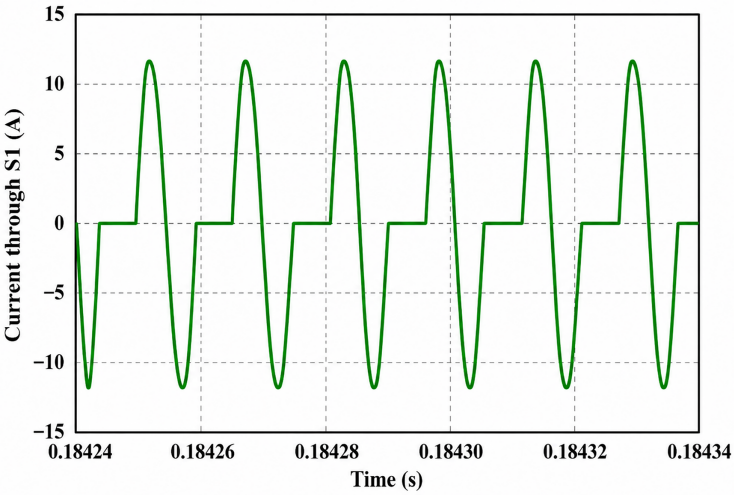


Figure 18: Current through switch Q_3.

The current wave-form through switches Q_2 and Q_4 are shown in Figs. 19 and 20. This current guarantees that during the complementary switching interval, AC will continually excite the resonant tank. Battery health is the prevention of DC bias in the battery and balanced current sharing made possible by switch pairs alternate conduction.

Fig. 21 shows the resonant inductor current (i_{Lr}) in the heating mode. The waveform is almost sinusoidal, indicating that L_r and C_r are in proper resonance. Through internal resistance, this resonant current directly adds to the battery's internal heat production. Stable heating without undue electrical stress is ensured by its smooth profile.

The voltage across the capacitor during heating operation is depicted in Fig. 22. Proper energy exchange within the resonant tank is shown by the capacitor voltage's smooth oscillating pattern. This voltage behavior guarantees controlled heating current generation with low losses and validates stable resonant functioning.

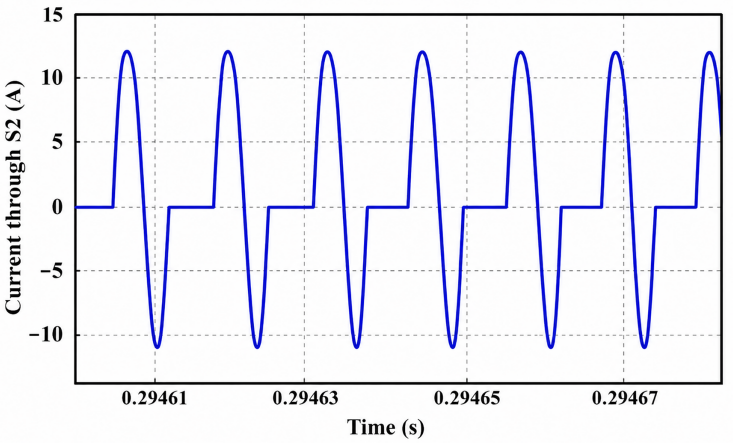


Figure 19: Current through switch Q_2.

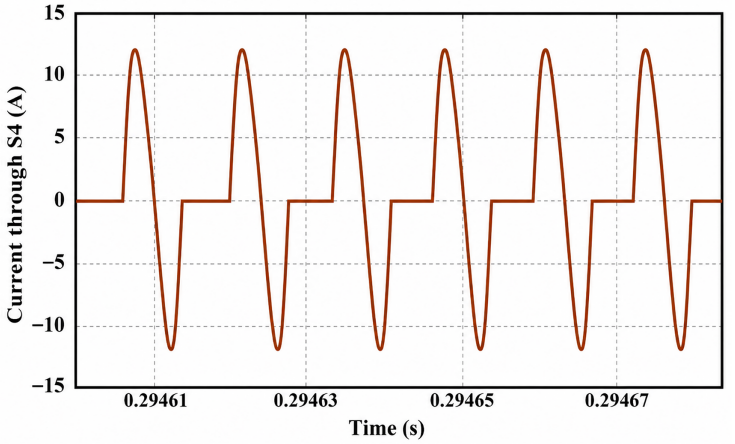


Figure 20: Current through switch Q_4.

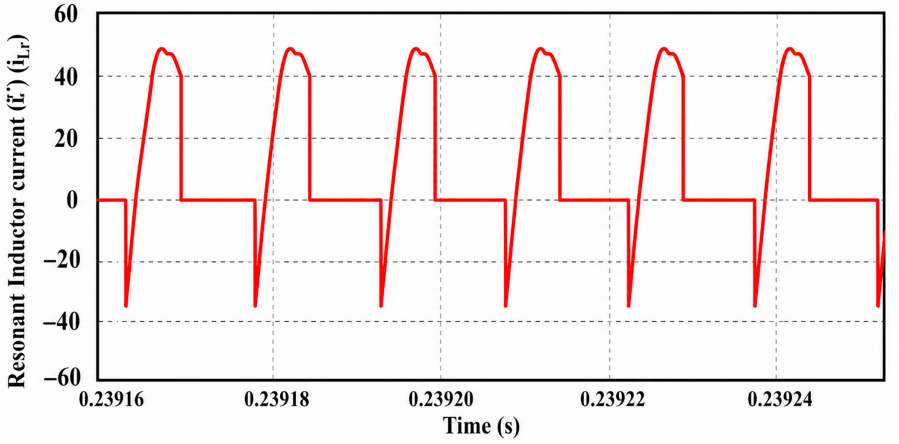


Figure 21: Resonant inductor current i_{Lr} during heating mode.

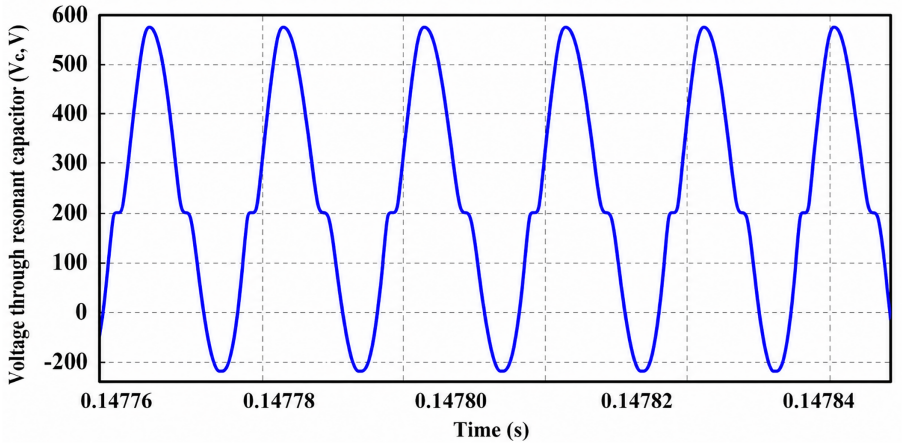


Figure 22: Voltage across resonant capacitor C_r in heating mode.

It is clear from the obtained simulation results that the proposed converter effectively generates a controlled alternating current through the battery during the heating mode. The proposed topology is suitable for low-temperature EV applications, as the soft-switching operation, resonant current shaping, and balanced switch operation contribute to efficient and reliable battery heating. The simulation results demonstrate stable operation and effective control of the AC battery heating current under different operating conditions. The resonant current exhibits a near-sinusoidal waveform, confirming the resonant operation of the converter. Furthermore, the voltage and current waveforms demonstrate that the desired soft-switching conditions are achieved.

5 Experimental Validation

To check the feasibility of the suggested converter, a hardware prototype of the converter was built and tested under rated operational conditions. The results obtained prove the fact that the proposed converter works successfully both ways and also maintains soft switching behavior. The waveform presented in Fig. 23 depicts the waveforms for the gate signal and corresponding switch voltage.

It is clear from Fig. 23 that the switch voltage approaches near zero before switching on the device. Thus, the operation of the ZVS topology is confirmed. The experimentally measured waveform shows good agreement with the corresponding simulation waveform, indicating reduced switching losses under the tested operating conditions. The current waveform appears almost sinusoidal, which shows proper operation of the inductor with the capacitor. The waveforms obtained for voltage and current of the transformer from Fig. 24 demonstrate the effective transfer of power via the high-frequency transformer. The waveform proves the proper working of the transformer and the effective transfer of energy from the primary to secondary of the converter.

Fig. 25 shows the experimental wave form obtained in the battery heating mode. The observed resonant current waveform indicates that an alternating current is injected into the battery, with no significant DC component observed under the tested operating conditions. This validates the proposed AC heating approach for improving battery performance at low temperatures. Table 2 presents a comparison of the proposed converter with recently reported converters. The comparison demonstrates that the proposed converter integrates bidirectional power transfer and AC battery heating functionality within a single converter configuration while achieving soft-switching operation. In contrast to several existing resonant

converters that require an additional battery-heating circuit, the proposed converter provides a compact and integrated solution.

Table 3 illustrates the comparative analysis between the proposed converter and existing topologies considering the features, performance, and modulating methods. Most of the proposed topologies utilize one converter or battery heating circuits separately. The major advantage offered by the proposed converter is the provision of an integrated battery heating in the converter only which leads to compact and efficient design.

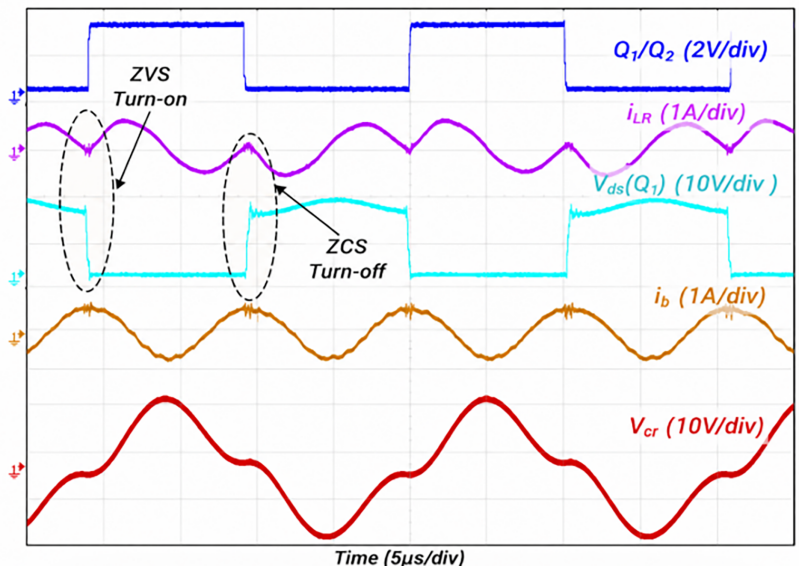


Figure 23: Experimental results for battery heating mode.

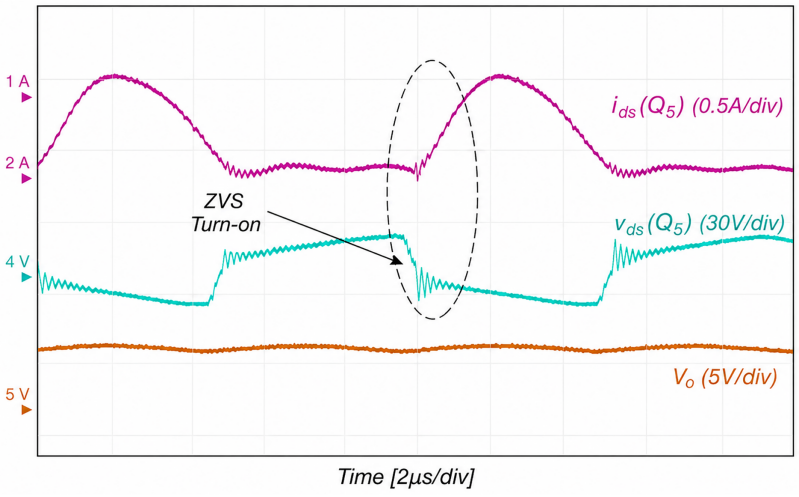


Figure 24: Experimental results for transformer voltage and current.

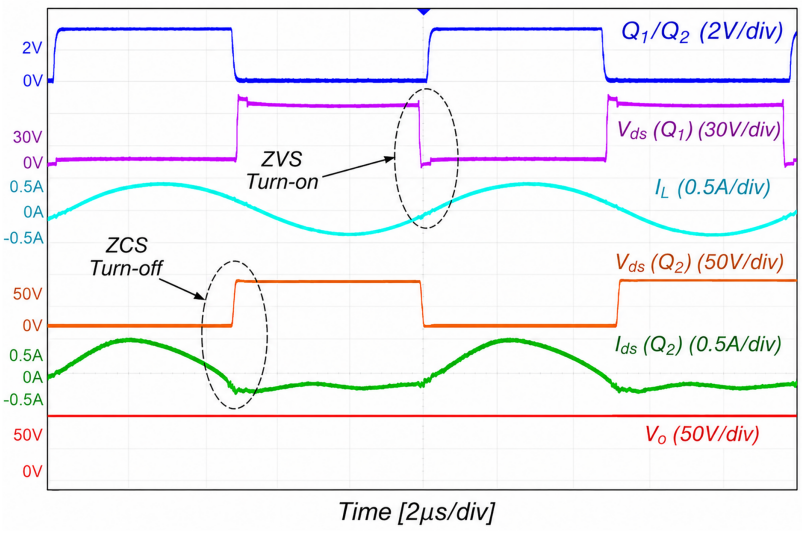


Figure 25: Experimental results for power transfer mode.

Table 2: Comparison with recent literature.

Reference	Bidirectional	Battery Heating	Reconfigurable	Soft Switching	Experimental Validation
Khan et al. (2026) [14]	✓	X	✓	ZVS	✓
Li et al. (2022) [24]	✓	X	✓	ZVS	✓
Luo et al. (2025) [20]	✓	X	X	ZVS	✓
Proposed Work	✓	✓	✓	ZVS/ZCS	✓

Note: Abbreviation: ZVS—Zero voltage switching; ZCS—Zero current switching.

Table 3: Comparison between the proposed converter with recent converter topologies.

Resonant Topologies	[13]	[17]	[14]	[20]	[22]	Proposed
Output Power	1 kW	500 W	350 W	2.5 kW	500 W	1 kW
Switching Frequency	80–160 kHz	170–260 kHz	55–110 kHz	80–140 kHz	100 kHz	80–180 kHz
Gain	1.2–2.1	1.3–1.8	1.3–1.5	0.5–1.1	0.4–1.8	0.8–2.6
Efficiency	92.15	90.7	91.42	91.25	91.75	92.23%
Number of switches and diodes	6	4 switches & 2 diodes	2 switches & 4 diodes	4 switches & 4 diodes	7 switches & 3 diodes	12 switches
Inductors count	4	2	4	3	2	2
Capacitors count	2	1	2	2	1	2
Transformers count	2	1	2	1	1	1

6 Conclusion

In this paper, the bidirectional resonant DC-to-DC converter with a built-in battery heating mechanism for use in EVs was introduced. In the proposed design, both the capability of bidirectional power conversion and AC heating of the battery have been incorporated into one converter configuration. As a result, the hardware system is simplified, and an additional battery-heating circuit becomes unnecessary. Stable operation of the converter was experimentally and numerically demonstrated in both operating modes—power conversion and battery heating. The performance of the proposed converter was analyzed under different load and battery voltage conditions. The converter's efficiency is 92.3% when it is operating at its highest point. The efficiency is also achieved through soft switching throughout its operating range. The adaptive LLC/LLCC reconfiguration expands the voltage gain without imposing too high a switching frequency; thus, lower switching losses are achieved. Experimental measurements proved that ZVS switching, stable resonant current, and bi-directionality were achieved, thus confirming the simulations. The suggested frequency modulation control algorithm provides mode transition and resonant operation of the converter over a wide range of battery voltage. It is scalable for high-power EV applications owing to its modular configuration and flexible control algorithm. Future work will focus on detailed electro-thermal battery analysis, efficiency optimization under different loading conditions, and comprehensive long-term experimental evaluation using high-power EV battery systems.

Acknowledgement: Not applicable.

Funding Statement: The authors received no specific funding for this study.

Author Contributions: Indira Damarla: conceptualization, investigation, writing—original draft, writing—review & editing. Subhojit Dawn: conceptualization, investigation, writing—original draft, writing—review & editing. Ramudu Ganji: conceptualization, investigation, writing—original draft, writing—review & editing. Venmathi Mahendran: conceptualization, investigation, writing—original draft, writing—review & editing. Taha Selim Ustun: conceptualization, investigation, writing—original draft, writing—review & editing. All authors reviewed and approved the final version of the manuscript.

Availability of Data and Materials: Data is available from the corresponding authors upon reasonable request.

Ethics Approval: Not applicable.

Conflicts of Interest: The authors declare no conflicts of interest.

References

1. Tappeta VSR, Appasani B, Patnaik S, Ustun TS. A review on emerging communication and computational technologies for increased use of plug-in electric vehicles. Energies. 2022;15(18):6580. doi:10.3390/en15186580.
2. Kumar RR, Bharatiraja C, Udhayakumar K, Devakirubakaran S, Sekar KS, Mihet-Popa L. Advances in batteries, battery modeling, battery management system, battery thermal management, SOC, SOH, and charge/discharge characteristics in EV applications. IEEE Access. 2023;11:105761–809. doi:10.1109/ACCESS.2023.3318121.
3. Jaguemont J, Boulon L, Venet P, Dubé Y, Sari A. Lithium-ion battery aging experiments at subzero temperatures and model development for capacity fade estimation. IEEE Trans Veh Technol. 2016;65(6):4328–43. doi:10.1109/TVT.2015.2473841.
4. Sun Q, Lv H, Wang S, Gao S, Wei K. Optimized state of charge estimation of lithium-ion battery in SMES/battery hybrid energy storage system for electric vehicles. IEEE Trans Appl Supercond. 2021;31(8):5700606. doi:10.1109/TASC.2021.3091119.
5. Zhu J, Sun Z, Wei X, Dai H, Gu W. Experimental investigations of an AC pulse heating method for vehicular high power lithium-ion batteries at subzero temperatures. J Power Sources. 2017;367:145–57. doi:10.1016/j.jpowsour.2017.09.063.

6. Shang Y, Liu K, Cui N, Zhang Q, Zhang C. A sine-wave heating circuit for automotive battery self-heating at subzero temperatures. IEEE Trans Ind Inf. 2020;16(5):3355–65. doi:10.1109/tii.2019.2923446.
7. Zhao Z, Xu J, Liu Z, Zou Z, Mei X. An automotive onboard self-heating method based on reconfigurable battery system in cold climates. IEEE Trans Ind Inf. 2025;21(9):6799–810. doi:10.1109/tii.2025.3567399.
8. Zhu C, Cao Y, Zhang H, Lu F, Zhang X. Comprehensive design and optimization of an onboard resonant self-heater for EV battery. IEEE Trans Transp Electrific. 2021;7(2):452–63. doi:10.1109/tte.2020.3025014.
9. Shang Y, Liu K, Cui N, Wang N, Li K, Zhang C. A compact resonant switched-capacitor heater for lithium-ion battery self-heating at low temperatures. IEEE Trans Power Electron. 2020;35(7):7134–44. doi:10.1109/TPEL.2019.2954703.
10. Nagabushanam KM, Mahto T, Tewari SV, Udumula RR, Alotaibi MA, Malik H, et al. Development of bi-directional switched-capacitor DC-DC converter for EV powertrain application. Eng Sci Technol Int J. 2025;65:102016. doi:10.1016/j.jestch.2025.102016.
11. Guan Y, Wang Y, Wang W, Xu D. A high-frequency CLCL converter based on leakage inductance and variable width winding planar magnetics. IEEE Trans Ind Electron. 2018;65(1):280–90. doi:10.1109/TIE.2017.2716878.
12. Pi L. Modified two-channel LLC resonant converter with optimal efficiency for wide input voltage applications. IEEE Access. 2023;11:38957–69. doi:10.1109/ACCESS.2023.3267851.
13. Wang C, Yang L, Wang Y, Chen B. A 1-kW CLTCL resonant DC-DC converter with restricted switching loss and broadened voltage range. IEEE Trans Power Electron. 2018;33(5):4190–203. doi:10.1109/TPEL.2017.2719162.
14. Khan MM, Wagaye TA, Temesgen ES, Kang DY, Kim M. Reconfigurable bidirectional interleaved neutral-point-clamped resonant DC/DC converter for high and wide voltage gain range. IEEE Trans Ind Electron. 2026;73(7):9932–46. doi:10.1109/TIE.2025.3642426.
15. Khan S, Chub A, Bakeer A, Vinnikov D, Kasper MJ, Deboy G. A comprehensive review of galvanically isolated DC-DC converters for wide voltage gain range applications. IEEE Open J Power Electron. 2026;7:1177–216. doi:10.1109/OJPEL.2026.3679212.
16. Chen B, Wang P, Wang YF, Zhang SH, Yang L, Ji RL. A bidirectional CDT-LC resonant DC–DC converter with a wide voltage range. IEEE Trans Ind Electron. 2020;67(3):2009–20. doi:10.1109/tie.2019.2907504.
17. Jovanovic MM, Irving BT. On-the-fly topology-morphing control—efficiency optimization method for LLC resonant converters operating in wide input- and/or output-voltage range. IEEE Trans Power Electron. 2016;31(3):2596–608. doi:10.1109/tpel.2015.2440099.
18. Queiroz SS, Costa LF. LLC resonant converter with reconfigurable secondary-side for output voltage regulation. IEEE Trans Circuits Syst II Express Briefs. 2025;72(12):2047–51. doi:10.1109/TCSII.2025.3625415.
19. Lu X, Wang H. A highly efficient multifunctional power electronic interface for PEV hybrid energy management systems. IEEE Access. 2019;7:8964–74. doi:10.1109/ACCESS.2018.2889099.
20. Luo X, Yao X, Wang J, Ma H, Huang S, Liao Y. A three-leg reconfigurable *LLC* resonant converter for wide-voltage-gain application. IEEE J Emerg Sel Topics Power Electron. 2025;13(6):6945–57. doi:10.1109/jestpe.2025.3577284.
21. Reddy RM, Das M. Reconfigurable dual output resonant DC–DC converter for wide output voltage applications. IEEE Trans Transp Electrific. 2025;11(1):1004–14. doi:10.1109/tte.2024.3399608.
22. Shen Y, Wang H, Al-Durra A, Qin Z, Blaabjerg F. A structure-reconfigurable series resonant DC–DC converter with wide-input and configurable-output voltages. IEEE Trans Ind Applicat. 2019;55(2):1752–64. doi:10.1109/tia.2018.2883263.
23. Ren C, Qin Y, Kong J, Li X, Hui Y, Han X, et al. A triple-LC-based DC/DC converter with wide input voltage gain in both under-resonance and over-resonance frequency regions. IET Power Electron. 2024;17(14):1761–71. doi:10.1049/pel2.12731.
24. Li G, Yang D, Zhou B, Liu YF, Zhang H. Integration of three-phase LLC resonant converter and full-bridge converter for hybrid modulated multioutput topology. IEEE J Emerg Sel Topics Power Electron. 2022;10(5):5844–56. doi:10.1109/jestpe.2021.3139905.
25. Tran HN, Nguyen LHB, Vo MV, Nguyen TD. A non-Ecap wide range bidirectional OBC with multifunction circuit. IEEE Trans Transp Electrific. 2026;12(4):6897–907. doi:10.1109/tte.2026.3680312.